

**Impact of Topography on Molecular-Beam Scattering on Surfaces: The NO-Diamond Case**C. Flytzanis,<sup>(a)</sup> H. Kuze,<sup>(b)</sup> M. Chatelet,<sup>(a)</sup> J. Häger, and H. Walther*Max-Planck-Institut für Quantenoptik, D-8046 Garching, Federal Republic of Germany*

(Received 31 March 1988)

State-selective laser techniques are used to study the scattering of NO molecules on a crystallographic diamond surface. It is inferred that the diamond surface differentiates between "left" and "right" incoming molecules and accordingly endows them with different energy contents after the collision without providing any energy to them. Time-of-flight spectra show the existence of two velocity components in the scattered molecules that correspond to two different molecule-surface collision histories.

PACS numbers: 79.20.Rf, 68.45.Da, 82.65.My, 82.65.Pa

We present the first experimental study of molecular-beam scattering on a crystallographic diamond surface using state-selective laser techniques. These techniques<sup>1-6</sup> allow one to prepare the molecules in well-defined states of internal and translational motion before their interaction with the surface, and, by interrogating their state after the collision, to deduce essential features of the dynamics of the molecule-surface interaction as well as the energy transfer and accommodation that takes place among the single molecule and the surface degrees of freedom. This problem is particularly intriguing<sup>1,7</sup> compared with the one occurring in molecule-molecule collisions since the degrees of freedom of the two interacting partners, the single molecule and the surface, are of fundamentally different character, individual and collective, respectively.

The choice of diamond in our case contrasts in many essential physical aspects with previous similar studies on graphite, its allotrope carbon partner, and other crystalline surfaces, metallic or dielectric, because of the singular position that diamond occupies<sup>8,9</sup> among crystals. In order to appreciate the distinct features in the molecule-surface interaction that one may anticipate here, it suffices to state that the unreconstructed diamond surface possesses no inversion symmetry while the graphite surface does, as do also the other close-packed metallic and ionic crystalline surfaces studied<sup>1</sup> up till now. Furthermore, the Debye temperature of diamond is exceptionally high,  $\Theta_D \approx 2200$  K for the bulk and  $\Theta_D \approx 1800$  K for the surface, a unique case in solid-state physics, all other crystals having values for  $\Theta_D$  close to the room temperature: Accordingly, the amplitude<sup>9</sup> of the mean thermal motion of the surface carbon atoms is almost 1 order of magnitude smaller in diamond than in any other crystal and does not smear out the surface features.

The experimental technique and setup have already been described in connection with the investigation on graphite.<sup>2,6</sup> For completeness we remind the reader that the scattering and diagnostics take place in an ultra-high-vacuum (UHV) chamber. A pulsed supersonic beam of NO molecules, optionally seeded by helium, is

scattered from a diamond surface in the center of the UHV chamber held at a background gas pressure of  $10^{-10}$  mbar. The surface ( $6 \times 4$  mm<sup>2</sup>) was obtained by the polishing of a type-IIa diamond along the (111) surface as checked by von Laue back diffraction and the subsequent cleaning of it. Throughout the preparation stage and the experiments, the surface temperature never exceeded 1000 K, so that we worked with an unreconstructed surface;<sup>10-12</sup> no surface contamination was detectable by Auger electron spectroscopy. The translational energy of the rotationally cool ( $T_{\text{rot}} \approx 20$  K) incoming molecules can be varied with a small velocity spread in the range of 700–2800 cm<sup>-1</sup> by variation of the NO:He ratio.

The scattered molecules are interrogated with a pulsed, tunable, frequency-doubled dye laser pumped by an excimer laser, and the rotational energy distribution is determined by the relative intensity of the resonantly enhanced two-photon ionization signal as the laser frequency is varied; this diagnostic combined with a time-of-flight technique and a rotatable quadrupole mass spectrometer allows one to measure state-selective angular, rotational, vibrational, and velocity distributions of the scattered NO molecules for different incident angles  $\theta_i$  and surface temperatures  $T_s$  ranging from 200 up to 700 K. For the case of diamond, it was imperative that the measurements be repeated for two orientations of the sample, obtained by turning it by 180°; below they will be arbitrarily referred to as "left" and "right."

The most striking revelation of this dual series of measurements, and a confirmation of our anticipation concerning the impact of the diamond surface topography, is the left-right asymmetry exhibited in the angular distribution of the scattered molecules as recorded with the mass spectrometer and depicted in Fig. 1. In the case of the faster incident molecules in particular, the single narrow lobe obtained in one direction contrasts with the broader and apparently double lobe recorded in the opposite direction. This can be traced back to specific features of the topography and dynamics of the diamond surface, which are nonexistent or suppressed in the graphite surface.

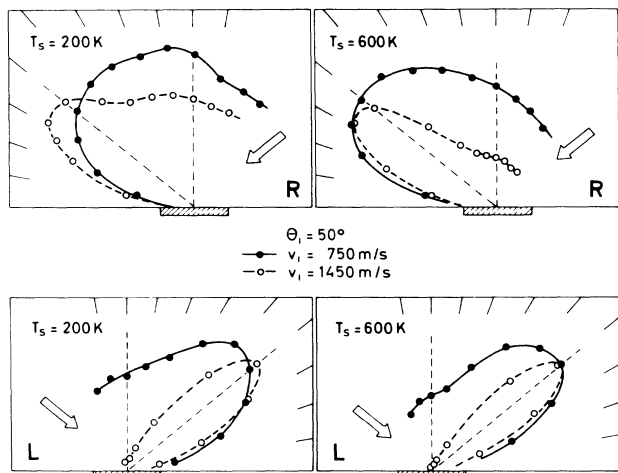


FIG. 1. Right (R) and left (L) scattering asymmetry for two surface temperatures and incident velocities.

The diamond structure and its (111)-surface termination are schematically depicted in Fig. 2 and compared with the graphite structure. The (111) surface is the plane of easiest cleavage as it requires the breaking of the smallest number of bonds per unit area. It is well ordered<sup>9-12</sup> and bulklike and shows neither reconstruction (parallel displacements of atoms) nor relaxation (perpendicular displacement of atoms) up to 1000 K. Up to this temperature the dangling bonds are actually terminated<sup>10-12</sup> with hydrogen atoms which start evaporating when the temperature is raised above 1000 K and reconstruction gradually sets in; the process completes at  $\sim 1200$  K. Because of the very tight C-H bonding the hydrogenation stabilizes the surface carbon atoms at their bulklike positions and hinders reconstruction, but otherwise has a very minor effect on the electronic distribution and may be momentarily disregarded.

Referring again to Fig. 2, because of the difference in the chemical bonding, the uppermost plane of the graphite surface is a regular planar array of strictly planar carbon hexagons, with all six carbon atoms equivalent, and possesses the inversion symmetry, while the diamond (111) surface does not. This bulklike surface when looked at from above also appears as a regular array of hexagons, but which are tilted and not planar; indeed, the atoms alternate around each ring in an upper (the hydrogenated) and a lower position, each group of three equivalent atoms forming an isosceles triangle. By oversimplification of the electronic density distribution, the surface profile along any of the three equivalent directions of the (111) surface has a sawtooth appearance with asymmetric triangular "grooves," schematically depicted in Fig. 2 with a simplified scattering geometry.

Accordingly, the diamond surface is not centrosymmetric and presents a different profile to left and right

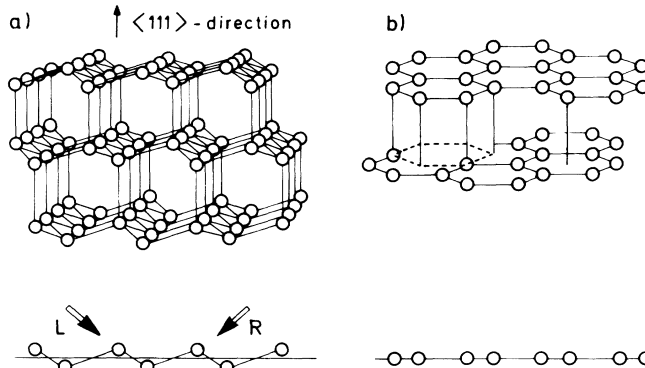


FIG. 2. Schematics of the (a) diamond and (b) graphite structures. The asymmetric profile of the diamond (111) surface and the hexagonal channels (in a different but equivalent surface) are demonstrated.

incoming molecules; the observed L-R asymmetry in the scattering profiles as revealed in Fig. 1 bears the signature of this topographic feature. Furthermore, as can be seen from Fig. 2, the crater-shaped hexagons, each with the three higher-lying hydrogenated carbon atoms, may act as geometrical traps, with pronounced asymmetry in the time periods that they geometrically accommodate incoming molecules.

The different left and right angular scattering distributions also underlie different energy distributions. In Fig. 3 we show two typical time-of-flight traces, for left and right incoming molecules. As can be seen there, the flux profiles for a given rotational level  $J$  in general consist of two components, a sharp one and a broader one corresponding, respectively, to specularly and diffusively scattered molecules in the angular distribution, with the broader one showing a substantially long residence time on the surface: approximately 0.1–0.5 ms, which was measured by our delaying the laser pulse with respect to the molecular-beam pulse. The relative importance of the two components differs for the left and right incoming molecules and, in addition, depends on the surface temperature  $T_s$  [Fig. 3(R)], the rotational state  $J$  [Fig. 3(L)], and the exit angle  $\theta_s$ . The slow component does not obey a  $\cos\theta$  distribution law but shows a R-L asymmetry. It was found that the sharp component is dominant for the L incoming molecules, whereas the broad component is dominant for the R incoming ones, and this accounts for the more pronounced double lobe previously pointed out in Fig. 1 for the scattering profile of these molecules.

We attribute the sharp component to the fast molecules that only experience a single (or eventually double) hard (elastic) collision on the overall rigid diamond (111) surface and are predominantly scattered in the specular direction. For these molecules we expect an efficient transfer of energy from translation to rotation. We attribute the broad component to molecules that are

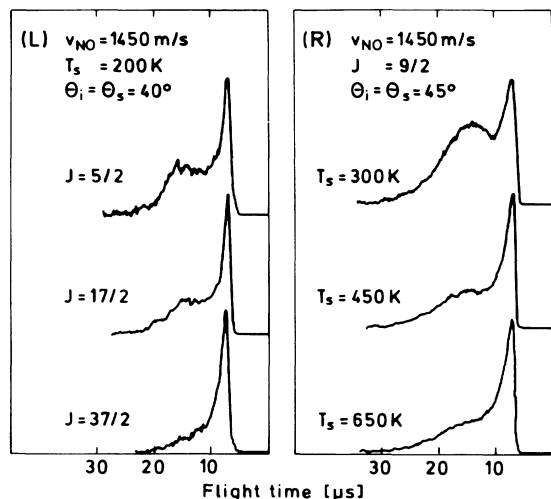


FIG. 3. Time-of-flight profiles for R and L scattering geometry for different surface temperatures and rotational states of the scattered particles, respectively.

“geometrically” trapped and accommodated for a long period of time inside the craterlike corrugations on the diamond (111) surface, where they experience a complex motion before they reemerge considerably slowed down and in directions that to a certain extent reflect the geometry of the traps; the asymmetric angular distribution of this component, clearly exhibited in Fig. 1, supports this picture.

As can be seen in Fig. 4, the scattered molecules of the slow component emerge in a rotational Boltzmann distribution corresponding to a  $T_{\text{rot}} \approx 380$  K which is independent of the surface temperature  $T_s$  and the incident and exit angles  $\theta_i$  and  $\theta_s$ , respectively. Those of the fast component emerge in an overall rotational energy distribution that also can be described by a Boltzmann distribution but with a rotational temperature markedly higher than that of the slow component, and which also does not depend on  $T_s$  but does depend on the incident angle  $\theta_i$ ; here, however, a small number of high- $J$  molecules show a deviation from a strict Boltzmann plot, indicating the onset of rotational rainbow scattering. It was checked and found that these rotational temperatures are identical for the two ground electronic states of the NO molecule,  ${}^2\Pi_{1/2}$  and  ${}^2\Pi_{3/2}$ . Also, the overall population ratio of these two electronic states,  $N({}^2\Pi_{1/2}) : N({}^2\Pi_{3/2})$  is given by  $\exp(\Delta E/T_{\text{rot}})$ , where  $\Delta E$  is the fine-structure splitting and  $T_{\text{rot}}$  is the rotational temperature for the fast or slow velocity component. This implies that each velocity component of the scattered molecules is rotationally and electronically in equilibrium characterized by  $T_{\text{rot}}$ .

The absence of any correlation between rotational and surface temperatures in the case of the fast velocity component, as shown in Fig. 4, is consistent with the assumption that the corresponding molecules only experience a

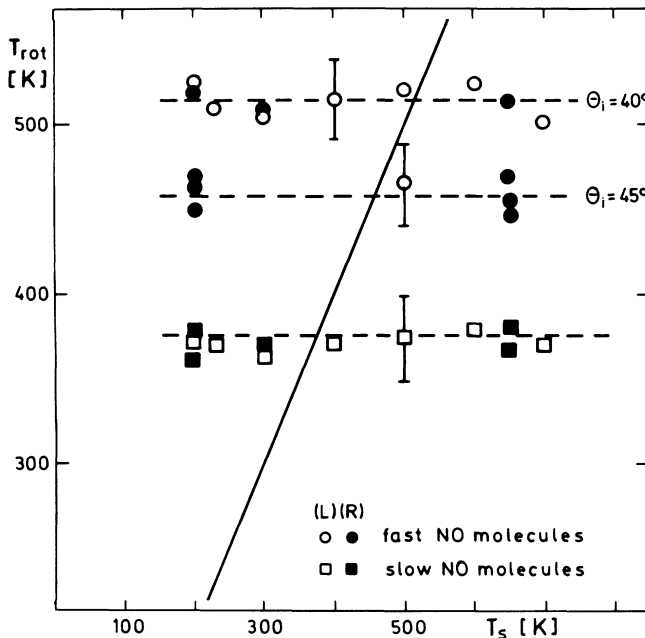


FIG. 4. Rotational temperature of slow and fast NO molecules vs surface temperature after scattering from the diamond (111) surface. Incident velocity,  $v_i = 1450$  m/s.

single collision with a rigid surface but do not exchange energy with it; on the other hand, the collision with a rigid surface provides<sup>13</sup> a very efficient coupling mechanism for translational and rotational modes. This is strikingly demonstrated in Fig. 5, which shows a complete correlation between a rotational-state-resolved measurement of the peak velocity of the fast molecules (or, equivalently, their peak kinetic energy  $E_{\text{kin}}$ ) and the rotational-state

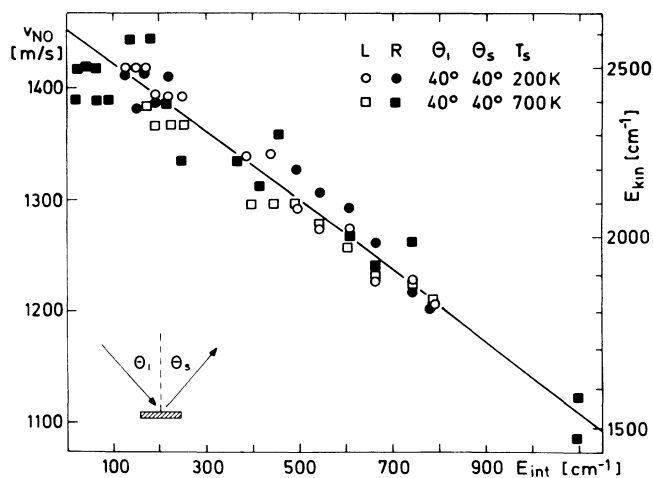


FIG. 5. Peak velocity vs internal energy  $E_{\text{int}}$  of the scattered NO molecules of the fast component for L and R scattering geometries and two surface temperatures. Incident velocity,  $v_i = 1450$  m/s.

energy  $E_{\text{rot}}$  expected by overall energy conservation for a sole molecule without energy exchange with the rigid surface, or  $E_{\text{kin}} + E_{\text{rot}} = \text{const}$ . This is in remarkable contrast to the results for the NO/graphite system, where the peak velocities were nearly independent of the rotational state.<sup>6</sup> In addition, the observed increase of  $T_{\text{rot}}$  as  $\theta_i$  decreases (the direction of incoming molecules approaches the normal), as shown in Fig. 4, indicates that the rotational energy gain that is experienced by the molecules of the fast component after their collision with the diamond surface occurs at the expense of the normal component of the incoming translational energy  $E_n = E_{\text{kin}} \cos^2 \theta_i$ , the tangential component being conserved as expected<sup>13</sup> for a hard collision on a rigid surface.

In contrast, it is difficult to give a detailed picture of the interaction history of the molecules of the slow component. Their long residence time on the surface (of the order of 0.1–0.5 ms) is attributed to geometrical trapping and accommodation of these molecules inside the craterlike corrugations, where they undergo a complex motion with multiple collisions with the hard walls of the corrugation before being ejected in the directions of easiest escape as imposed by the geometry of the traps and the dynamics of the interaction. Their rotational and translational energy distributions are fitted with Boltzmann and Maxwell distributions, respectively, and are both characterized by roughly the same temperature, 380 K. This indicates that each molecule only interacts locally with a single corrugation during its residence time, in “thermal” isolation from the rest of the surface. The geometrical trapping inside the corrugations of the diamond surface is quite distinct from adsorption or chemisorption processes. Since the dangling bonds are hydrogenated under our conditions, chemisorption should be inoperative; furthermore, chemisorption would lead to drastic alteration of the scattering patterns with time which we never observed. Physical adsorption is

also ineffective in diamond as the attractive surface potential is negligible.

The case of diamond opens the way to some novel experimental and theoretical investigations related to its specific topography and high Debye temperature. But this is not restricted to diamond only; it may well show up in other surfaces such as, in particular, unreconstructed covalent ones, semiconductors, or others.

<sup>(a)</sup>Permanent address: Laboratoire d'Optique Quantique, Ecole Polytechnique, 91128 Palaiseau Cedex, France.

<sup>(b)</sup>Permanent address: Department of Physics, Faculty of Liberal Arts, Shizuoka University, Shizuoka 422, Japan.

<sup>1</sup>For a review, see J. A. Barker and D. J. Auerbach, *Surf. Sci. Rep.* **4**, 1 (1985).

<sup>2</sup>F. Frenkel, J. Häger, W. Krieger, H. Walther, C. T. Campbell, G. Ertl, H. Kuipers, and J. Segner, *Phys. Rev. Lett.* **46**, 152 (1981).

<sup>3</sup>G. M. McClelland, G. D. Kubiak, H. G. Rennagel, and R. N. Zare, *Phys. Rev. Lett.* **46**, 831 (1981).

<sup>4</sup>M. Asscher, W. I. Guthrie, T. H. Lin, and G. A. Somorjai, *Phys. Rev. Lett.* **49**, 76 (1982).

<sup>5</sup>H. Zacharias, M. M. T. Loy, and P. A. Roland, *Phys. Rev. Lett.* **49**, 1790 (1982).

<sup>6</sup>J. Häger, Y. R. Shen, and H. Walther, *Phys. Rev. A* **31**, 1962 (1985).

<sup>7</sup>See, for instance, C. W. Mühlhausen, L. R. Williams, and J. C. Tully, *J. Chem. Phys.* **83**, 2594 (1985).

<sup>8</sup>N. W. Ashcroft and N. D. Mermin, *Solid State Physics* (Holt-Saunders, Tokyo, 1981).

<sup>9</sup>R. Berman, *Physical Properties of Diamond* (Oxford Univ. Press, New York, 1965).

<sup>10</sup>P. G. Lurie and J. M. Wilson, *Surf. Sci.* **65**, 453 (1977).

<sup>11</sup>T. E. Derry, L. Smit, and J. F. van der Veen, *Surf. Sci.* **167**, 502 (1986).

<sup>12</sup>B. B. Pate, *Surf. Sci.* **165**, 83 (1986).

<sup>13</sup>W. Nichols and J. M. Weare, *J. Chem. Phys.* **62**, 3754 (1975), and **66**, 1075 (1977).